

**University of California**

**Ernest O. Lawrence  
Radiation Laboratory**

**TWO-WEEK LOAN COPY**

*This is a Library Circulating Copy  
which may be borrowed for two weeks.  
For a personal retention copy, call  
Tech. Info. Division, Ext. 5545*

**MEASUREMENT OF ABSORPTION LINE PROFILES  
WITH A FABRY-PEROT INTERFEROMETER**

**Berkeley, California**

## **DISCLAIMER**

This document was prepared as an account of work sponsored by the United States Government. While this document is believed to contain correct information, neither the United States Government nor any agency thereof, nor the Regents of the University of California, nor any of their employees, makes any warranty, express or implied, or assumes any legal responsibility for the accuracy, completeness, or usefulness of any information, apparatus, product, or process disclosed, or represents that its use would not infringe privately owned rights. Reference herein to any specific commercial product, process, or service by its trade name, trademark, manufacturer, or otherwise, does not necessarily constitute or imply its endorsement, recommendation, or favoring by the United States Government or any agency thereof, or the Regents of the University of California. The views and opinions of authors expressed herein do not necessarily state or reflect those of the United States Government or any agency thereof or the Regents of the University of California.

Submitted to the  
Journal of the Optical Society of America

UCRL-16262

UNIVERSITY OF CALIFORNIA  
Lawrence Radiation Laboratory  
Berkeley, California

AEC Contract No. W-7405-eng-48

MEASUREMENT OF ABSORPTION LINE PROFILES  
WITH A FABRY-PEROT INTERFEROMETER

Robert J. Hull and Lee C. Bradley, III

May 3, 1966

MEASUREMENT OF ABSORPTION LINE PROFILES  
WITH A FABRY-PEROT INTERFEROMETER\*

Robert J. Hull<sup>†§</sup>

Lawrence Radiation Laboratory and Physics Department  
University of California, Berkeley, California  
and

Lee C. Bradley, III<sup>\*\*</sup>

MIT Lincoln Laboratory, Lexington 73, Massachusetts

May 3, 1966

ABSTRACT

We have calculated the line profiles to be expected when a Fabry-Perot interferometer is used to measure absorption lines. We have shown that large errors may be introduced in the measurement of the integrated absorption, even when an interferometer of high finesse is used. Curves and tables are given for finding the true absorption width and the true peak absorption from the apparent values observed under different operating conditions of the emission light source and the interferometer. We show qualitatively that the distortions are partially due to the presence of nonzero wings in the instrument bandpass function. Finally, we show a Fourier series expansion of the integral giving the transmittance of the Fabry-Perot interferometer when absorbing atoms are present in the light path.

## INTRODUCTION

A basic problem in determining the true shape of a line in the absorption spectrum of a gas is how to take into account the effects of the instrument used in the measurement. In general, instruments tend to broaden the width while depressing the peak value of the absorption coefficient. We calculated the extent of these effects when they were caused by a Fabry-Perot interferometer. These calculations are similar to those performed by Kostkowski and Bass<sup>1</sup> for diffraction grating instruments whose instrument or slit functions were assumed to be either Gaussian or Lorentzian functions. More recently, Kyle and Green<sup>2</sup> have extended the calculations of Kostkowski and Bass for Gaussian slit functions to a wider range of conditions.

A direct approach to measuring an absorption line profile is to use a spectrometer whose resolving power is sufficient to trace out the absorption line as a function of frequency, and then to calculate the desired parameters from the experimentally observed emission and absorption line profiles. However, unless the spectrometer does not change the frequency distribution of the input light, there is no guarantee that the observed absorption line will bear any resemblance to the true line.

In the following discussion we shall show how the absorption coefficient profile is affected by a Fabry-Perot interferometer, with the effect shown as a function of the finesse and resolving power of the latter. The effects of varying the peak absorption and the ratio of the emission line width from the light source to absorption line

width are also calculated. Some experimental evidence for these calculated effects is presented. In Appendix A, a simplified representation of the transmittance of the Fabry-Perot brings home the main conclusions of this work with very little mathematics. Appendix B contains a derivation of a series expansion of the integral giving the transmittance of the Fabry-Perot interferometer when absorbing atoms are present in the light beam; this series converges fairly rapidly under some conditions and usually requires less computer time than a direct evaluation of the integral.

### CALCULATIONS

The advantages gained in using a Fabry-Perot interferometer rather than a diffraction-grating instrument are speed and compactness for a given resolving power. The ultimate resolving power achievable with a Fabry-Perot is usually greater than with other kinds of spectrometers. However, these advantages are partially offset by the problem of overlapping orders. Thus to use a Fabry-Perot interferometer for absorption line measurements, one must use a light source whose frequency spread corresponds to not more than one free spectral range of the interferometer. In laboratory work (as opposed to, say, astronomical or astrophysical work), the easiest way to achieve such a spread is by using a light source that contains a strong emission line at the wavelength of interest, and eliminating other emission lines by means of interference filters. This technique<sup>3</sup> was used to measure the absorption profiles of resonance lines of cesium and rubidium with the purpose of determining the density of atoms in the absorbing cell, when a value of the relevant lifetime is assumed.

If the input light to the absorbing medium has a frequency distribution given by  $f(\nu)$ , then the light of frequency  $\nu$  transmitted by the medium is given by

$$f(\nu) \exp[\kappa_T(\nu)]$$

where  $\kappa_T(\nu)$  is the true absorption coefficient. The effect of the interferometer used to analyze this light can be expressed as the convolution integral<sup>4</sup> of the above expression with the instrument function  $g(\nu)$ :

$$I_{\text{abs}}(\nu) = \int_{-\infty}^{\infty} f(\nu') \exp[-\kappa_T(\nu')] g(\nu - \nu') d\nu' . \quad (1)$$

In the absence of absorbing atoms, the output of the interferometer becomes

$$I_0(\nu) = \int_{-\infty}^{\infty} f(\nu') g(\nu - \nu') d\nu' . \quad (2)$$

The apparent absorption coefficient  $\kappa_A$  is then calculated by taking the natural logarithm of the ratio of the two outputs:

$$\kappa_A(\nu) = \ln \left[ \frac{I_0(\nu)}{I_{\text{abs}}(\nu)} \right] . \quad (3)$$

It is trivial to show that if the instrument function  $g(\nu - \nu')$  reduces to a delta function,  $\delta(\nu - \nu')$ , one indeed recovers the true absorption coefficient. In practice there is no simple relationship between the apparent and true profiles.

The Fabry-Perot has an instrument function given by the Airy function:

$$g(\nu) = \frac{1}{1 + \frac{4R}{(1-R)^2} \sin^2 \pi \nu} , \quad (4)$$

where  $R$  is the reflectivity of the interferometer plates, and  $\nu$ , the

frequency, is measured in units of one free spectral range. The free spectral range is equal to  $1/2t$ , where  $t$  is the separation between the plates. A figure of merit for the Fabry-Perot interferometer is the finesse  $N$ , which is defined as the ratio of the free spectral range to the observed width  $\Delta\nu$  at half-maximum of a monochromatic line broadened only by the instrument. For an ideal instrument with perfectly flat plates, finesse is determined by the reflectivity of the plates

$$N \cong \pi \sqrt{R}/(1 - R) . \quad (5)$$

In practice the instrumental width is always broader than this due to imperfections in the plates and the finite size of the detector.<sup>5</sup> Hence it is necessary to measure the instrumental width and use Eq. (5) to define an effective reflectivity for use in calculations. This procedure is not justifiable if the imperfections in the plates seriously change the instrument function. Incidentally, to measure<sup>6</sup> the true instrument width it is merely necessary to insert a narrow spacer (1 to 2 mm thick) to broaden the resolving limit of the Fabry-Perot. Then atomic emission lines become essentially monochromatic for this degraded instrument. The finesse is not changed by this procedure unless the plates are misaligned.

In these calculations, we evaluated integrals (1) and (2) numerically, using the Airy function as the instrument function. From the calculated values of  $I_0(\nu)$  and  $I_{\text{abs}}(\nu)$  and using Eq. (3), we obtained what we call apparent values for the various parameters describing the absorption coefficient: namely, the half-width  $a_A$ , defined as half the width of the apparent absorption coefficient at half its peak value; the intensity of the line,  $S_A$ , which is equal to the integral of the apparent absorption coefficient over the line, and the peak value  $\kappa_A^{\text{peak}}$  of the apparent absorption coefficient. These parameters will be distorted by the instrument

from their true values, which will be labeled with the subscript T. The light source or input line shape has been chosen as either a Gaussian of half-width  $a_E$  or as a rectangular pulse of constant intensity over one free spectral range and zero outside the range. This latter case might be achieved in practice in either of two ways: by running an emission line source in such a manner as to produce self-absorbed lines with relatively flat peaks, or by using a continuous light source in conjunction with a monochromator whose resolving limit is equal to the free spectral range of the interferometer. The absorption lines are taken to be Gaussians of the form

$$\kappa_T(\nu) = \kappa_T^{\text{peak}} \exp[-\ln 2(\nu/a_T)^2] . \quad (6)$$

We have then computed the deviations of the apparent parameters from the true ones, and how they depend on the following variables:

- a) the finesse of the Fabry-Perot interferometer,
- b) the ratio of the emission line width to absorption line width,
- c) the peak value of the absorption coefficient,  $\kappa_T^{\text{peak}}$ ,
- d) the ratio of interferometer resolving limit to absorption line half-width,  $\Delta\nu/a_T$ .

The integrals (1) and (2) were evaluated by either of two methods:

- a) a Simpson's rule numerical integration or
- b) the Fourier expansion as given in Appendix B.

The numerical computations were done on IBM computers. The Simpson's rule method required approximately 30 seconds on an IBM 7094 to obtain values of  $\kappa_A$  at 26 points across a free spectral range. Enough Fourier coefficients could be generated in 30 seconds on an IBM 1620 to calculate both  $I_0$  and  $I_{\text{abs}}$  to the same degree of accuracy as the Simpson's rule

method. Summing the two series required approximately an additional 3 seconds per point.

## RESULTS

The parameter least distorted by an instrument, as shown in the calculations of Kostkowski and Bass<sup>1</sup>, is the integrated absorption coefficient (line intensity). Table I gives some representative figures for the ratio of the apparent to true values of the integral as a function of the input emission line width and the resolving power of the Fabry-Perot, for a finesse of 25. The apparent line intensity varies from 0.9 to 27 times the true intensity, with the value depending on the conditions of operation. Similar results are obtained when  $\kappa_T^{\text{peak}}$  is allowed to vary. Thus Kostkowski and Bass's general conclusion that the integrated line intensity is conserved to a good approximation<sup>1</sup> is not at all valid for the Fabry-Perot interferometer.

This result can be ultimately traced to the shape of the Airy function in regions far from the peak. For a slit function that is either Gaussian or Lorentzian (as used by Kostkowski and Bass), the transmittance of the instrument eventually reaches vanishingly small limiting values far from the central maximum. However, the transmittance of an ideal Fabry-Perot does not drop to zero even for a reasonably good instrument. The ratio of peak to minimum transmission is  $(1+R)^2/(1-R)^2$ . The fact that this ratio is finite has the effect of producing transmission of light far from the line center. The apparent (computed) absorption coefficient ( $\kappa_A$ ) is plotted in Fig. 1 for a finesse of 50 and a ratio of instrument width to absorption width of  $\Delta\nu/a_T = 0.438$ ; and a ratio of 2.0 for the emission width to absorption width. For comparison we have plotted to the same

scale the "true" absorption coefficient ( $\kappa_T$ ) as a function of frequency. The wing in the transmittance of the Fabry-Perot has produced a tail in the apparent absorption coefficient. Thus, even for this particularly good interferometer, the area under  $\kappa$  has been exaggerated approximately 3 times. This effect probably would not be observed in practice for a Fabry-Perot of finesse 50 and moderate absorption ( $\kappa_T^{\text{peak}} \approx 1$ ). For the case considered, the difference between the transmitted intensities with and without absorption at the center of the pattern amounts to only 0.07% of the peak intensity. This small difference would undoubtedly be lost in noise in an experimental situation but does show up in the essentially noise-free computer calculation.

However, this type of behavior has been observed<sup>3</sup> in the laboratory when the finesse was as high as 30 and the  $\kappa_T^{\text{peak}}$  was approximately 2.0. Figure 2 is the recorded spectrum taken of the cesium  $D_1$  line with an interferometer of finesse 12 and an 8-mm spacer. The free spectral range for this instrument is  $0.625 \text{ cm}^{-1}$ , just about double the hyperfine splitting in the ground state of Cs. Each unresolved component is double due to the hf splitting of the excited state in this transition. The small dip in the center of Fig. 2 is the zero of light intensity. A mechanical shutter allowed light to alternately pass through and by pass the absorbing cell; thus the ac signal is a measure of the amount of absorption. The absorption between peaks is a real effect and is not due to improper normalization of the light intensity in the two beams. In the absence of absorbing atoms, the two light paths were adjusted to produce no observable difference in the fringes when the shutter flips back and forth between the two beams. The presence of absorbed light in the wings gives rise to the tail in the apparent absorption coefficient as it appears in the calculated profile of Fig. 1.

Similar behavior has also been observed in strontium experiments by Winocur and Pyle.<sup>7</sup> The absorption of light in the  $5^2S_{1/2} \rightarrow 5^2P_{1/2}$  transition of Sr II, occurring at 4216 Å, was monitored in a beam of strontium ions by a Fabry-Perot with  $N \approx 12$ . In these experiments there can be no question of false signals due to experimental technique, because only a single light path was used, the absorption being turned on and off either by interrupting the ion beam with a mechanical chopper or by pulsing the high voltage that produced the ions.

We tried to deduce the true absorption line intensity by measuring the area under  $\kappa_A$  out to the dip in its profile and out to where the difference between the intensities transmitted by the Fabry-Perot with and without absorption was less than 1% of the peak intensity. The latter criterion was chosen since absorption signals of this magnitude tended to be masked by noise in the experiments.<sup>3</sup> Neither method gave consistent estimates of the line intensity, and no correction factors were calculated.

The depression of the peak value of the absorption coefficient was regular. Hence correction factors were calculated for this parameter as a function of finesse, emission line width, and instrumental width. A typical set of computed data for a finesse of 25, plotted in Fig. 3, shows how the ratio  $\kappa_A/\kappa_T$  depends on the peak value of  $\kappa_T$  over the extremes of instrumental widths and emission line widths used in the calculations. The correction factors to be applied to  $\kappa_A$  then vary from about 1.1 to 5.0. The curves plotted in Fig. 3 are not particularly useful for generating corrections since the observable in an experiment,  $\kappa_A^{\text{peak}}$ , is not given explicitly. We have least-squares fitted the data from which these curves were plotted to a polynomial of second degree in  $\kappa_A^{\text{peak}}$  as follows:

$$\frac{\kappa_A^{\text{peak}}}{\kappa_T^{\text{peak}}} = a + b(\kappa_A^{\text{peak}}) + c(\kappa_A^{\text{peak}})^2. \quad (7)$$

Values of  $a$ ,  $b$ , and  $c$  are given in Table II for a finesse of 25. By using these tabulated values and Eq. (7), one can generate curves in which  $\kappa_A^{\text{peak}}$  is plotted versus  $\kappa_T^{\text{peak}}$ , for use in reducing other data. The region of validity of Eq. (7) is:

$$0 \leq \kappa_T^{\text{peak}} \leq 3.0 .$$

Over this range, values of  $\kappa_T^{\text{peak}}$  calculated from the parameters in Table II and Eq. (7) differ by less than 1% from the correct values.

We estimated the effect on  $\kappa_A^{\text{peak}}$  of varying the finesse of the interferometer about a mean value of 25. For these calculations, the spacing  $t$  between the Fabry-Perot plates was maintained constant while the finesse was varied from 22 to 28. This corresponds roughly to the experimental situation in which a given spacer is used in the etalon, but detuning occurs during the measurements, degrading the instrument. When the finesse changes by the  $\pm 12.0\%$  given above, the corrections to be applied to  $\kappa_A^{\text{peak}}$  vary by only  $\mp 5\%$ .

If, however,  $\Delta\nu/a_T$  is held fixed while the finesse is varied between 15 and 40, the correction factors then show a maximum spread of only  $\pm 1.4\%$  about their values for a finesse of 25. We conclude that  $\Delta\nu/a_T$  becomes the significant parameter, at least over a finesse range from 15 to 40. There is one precaution, however: For the low-finesse high-resolution case ( $N=15$ ,  $\Delta\nu/a_T = 0.438$ ), overlapping orders have begun to be a problem. The consistent results quoted above break down, and separate corrections must be applied. These corrections are not tabulated, since they depend strongly on the amount of overlap.

The corrections derived from Table II may be used over a finesse range of  $\approx 15$  to 40 and for  $0.875 \leq \Delta\nu/a_T \leq 4.38$ . The corrections in this table for  $\Delta\nu/a_T = 0.438$  apply only to a finesse of 25. The usefulness of the factors a, b, and c may be extended by graphical interpolation. By means of the data in the table, for example, a may be plotted versus  $\Delta\nu/a_T$ , with  $a_E$  used as a parameter or, alternatively, a versus  $a_E$  may be plotted with  $\Delta\nu/a_T$  as a parameter, and similarly for b and c. In this connection it is useful to remember that  $a = 1$  and  $b = c = 0$ , for  $\Delta\nu/a_T = 0$  or for  $a_E = 0$ . Hence a wide range of experimental conditions may be accommodated.

The ratio of apparent half-width to true half-width of the absorption line has been plotted in Fig. 4 as a function of  $\Delta\nu/a_T$ , again for an instrument of finesse 25 and when  $\kappa_T^{\text{peak}} = 0.3$ . The apparent width is very sensitive to the instrumental and emission-line widths. This result is in qualitative agreement with the work of Kostkowski and Bass.<sup>1</sup> If a reasonable assumption can be made for the absorption width to be expected in an actual experiment, as can be done for many laboratory situations, these curves may be used to cross check one's knowledge of the instrumental parameters.

Attempts to fit Gaussian curves to the computed (apparent) profiles proved fairly satisfactory for the narrow instrument widths ( $\Delta\nu/a_T = 0.438$  and 0.875). We used a simple two-parameter fit, matching the "fitted" Gaussian to the apparent profile at  $\kappa_A^{\text{peak}}$  and at the  $1/e$  point. This procedure produced a curve which agreed with the apparent profile to better than 5% at all intermediate points for  $\Delta\nu/a_T = 0.875$ , and to better than 2% for  $\Delta\nu/a_T = 0.438$ . An example of the apparent, fitted, and true profiles is plotted in Fig. 5. This process could be considered a

quantitative approximation to what one might try to do by eye--i. e., draw a curve through the observed points, extending it smoothly to zero, while neglecting the "tail." From the fitted Gaussians one can calculate a line intensity  $S_F$  and a width  $a_F$ . The ratios of these quantities to the true values are tabulated in Tables III and IV. Values of  $a_F/a_T$  given here agree with those plotted in Fig. 4, but are tabulated for a range of peak absorptions. Graphs useful to other workers can be obtained from the data given here.

One calculation was performed with a Voigt profile in absorption and a constant-intensity emission source. Our case corresponds to  $\kappa_T^{\text{peak}} = 0.3$ ,  $\Delta\nu/a_T = 0.438$ ,  $N = 25$ , and  $a = 0.7$ , where  $a$ , the natural damping ratio, is defined by Mitchell and Zemansky.<sup>8</sup> The apparent profile is plotted in Fig. 6 along with the apparent absorption line observed when a Gaussian input is used under the same conditions. The purpose of this calculation was to ascertain if a Fabry-Perot could be used to distinguish between the various kinds of absorption lines that might be observed in practice. From Fig. 6, we deduce that very careful experimental technique, when combined with a data analysis similar to that performed by Kuhn and Vaughan<sup>9</sup> on emission lines, could prove fruitful for simple absorption lines. However, a large signal-to-noise ratio would be necessary, especially in the wings of the line.

## APPLICATIONS

In order for one to use the results of this paper for a quantitative reduction of experimental data, considerable information concerning instrumental and absorption line parameters must be known in advance. The instrument width may be measured by using a narrow spacer and a

narrow atomic emission line as described above. An estimate of the half-width of the absorption line may often be made from the physical circumstances of the experiment. The width of the emission line can be measured using the Fabry-Perot interferometer and applying corrections such as those published by Minkowski and Bruck<sup>10</sup> or by Krebs and Sauer.<sup>11</sup> Thus values for  $\Delta\nu/a_T$  and  $a_E/a_T$  may be established.

Should the values of the ratios  $\Delta\nu/a_T$  and  $a_E/a_T$  not lie on one of the calculated curves, simple linear interpolation between the adjacent curves produces results of reasonable accuracy. This procedure has been checked and found to produce results within a few percent of the true values when these ratios lie near one of the curves. For higher accuracy, graphical interpolation may be used, as discussed earlier.

From the assumed values of  $a_T$  and the corrected value of  $\kappa^{\text{peak}}$ , the line intensity can be calculated for a Gaussian line, i. e., the shape to which our corrections apply. The plot of  $a_A/a_T$  may be used to roughly cross-check one's assumptions on either instrument width or absorption line width; but the curves are so steep that much reliance should not be placed on values deduced from this curve (Fig. 4).

Finally we should like to restate the assumptions under which the corrections deduced above are valid. First, the instrument function is taken to be a pure Airy function. The extent to which this assumption is valid in a particular case may be learned from Jacquinet's review article,<sup>5</sup> which summarizes the perturbations inherent in real Fabry-Perot interferometers. (See reference 3). Second, the absorption line is assumed to be Gaussian. This is often a good assumption, as Mitchell and Zemansky<sup>8</sup> show that the natural damping ratio  $a$  for some important resonance lines is small compared to one ( $a = 0$  means a pure Gaussian

line shape). We assume that the emission line may be approximated by a Gaussian line shape. This is probably not a very good assumption, since only under very special circumstances<sup>12</sup> would one expect an emission line to be pure Gaussian. However, the corrections to  $\kappa_A^{\text{peak}}$  are not very sensitive to the emission width. Hence this profile ought to give reasonable results and is simple to handle in computations.

Another very important assumption which has not been emphasized in these calculations is that there is only a single emission line and a single absorption line, centered on the emission line, present within one free spectral range of the combination of Fabry-Perot interferometer and predispersing element (interference filter, spectrometer, etc.). The interferometer is sensitive to light at all frequencies within its passband, and not merely to light whose frequency lies near the transmission peak of the instrument function. Serious errors may result, for example, if one were to apply these computations directly to absorption within, say, a hyperfine structure pattern.<sup>3</sup> The reason for this behavior will be made clear in Appendix A. This limitation to single emission and absorption lines may be modified if a number of simple lines overlap to such an extent that they appear as single lines even under infinite resolving power.

#### SUMMARY

Absorption line profiles observed with a Fabry-Perot interferometer are badly distorted from their true values. The Fabry-Perot does not conserve line intensity. Corrections to the peak value of the apparent absorption coefficient show a predictable, smooth variation under different conditions of illumination, instrumental finesse and width, and different peak absorptions. Hence under appropriate experimental conditions the

true value of the peak absorption coefficient may be determined to an accuracy of 10% or better. The parameters in Table II reproduce our calculations to better than 1% under the conditions specified.

#### ACKNOWLEDGMENTS

We wish to thank Professor Hyatt M. Gibbs for many valuable and stimulating discussions. Professor Howard A. Shugart gave much programming assistance during the early stages of the problem. Helpful suggestions for the preparation of the manuscript from Professors Sumner P. Davis and Herbert Kleiman are gratefully acknowledged. The computations were performed on the Berkeley Campus IBM 7090/7094 computer, the Lawrence Radiation Laboratory IBM 7094 computer, and the U. C. Physics Department IBM 1620.

## APPENDICES

A. Importance of the Wing in the Fabry-Perot Transmittance

Our main conclusions concerning the nonconservation of absorption line intensity by a Fabry-Perot interferometer and the depressions of the peak value of the absorption coefficient may be deduced from a simple picture of what the Fabry-Perot does to the input light. For this discussion we shall approximate the emission and absorption lines as rectangular functions of frequency. We take the emission line of constant intensity and of width 2.5 times the width of the absorption line and zero elsewhere. The absorption line, also rectangular, is centered on the emission line. The Airy function is approximated by a central rectangular peak of half the width of the absorption line. The wings of this instrument function are taken to be of constant intensity, one-tenth the intensity of the main peak. We shall not worry about the problem of overlapping orders and assume no other lines (emission or absorption) within the bandpass of this instrument.

The convolution integral is equivalent to placing the instrument function over the input spectrum, multiplying the two point-by-point, and integrating the resulting product function. This is a very simple procedure for the functions as we have chosen them. In order to be specific we have plotted the emission and absorption spectra and the instrument function in Fig. 7 to a frequency scale in which the emission line width is 10 units, the absorption width is 4 units, and the width of the central peak of the instrument function is 2 units. The emission line has a height of 2.0 units. The absorption coefficient is  $\kappa_T(\nu) = \kappa_T^{\text{peak}} = 0.288$  for  $4 \leq \nu \leq 6$  and is zero elsewhere. For this value, the center of the emission line in the input light is removed to a height of 1.5. The height of the instrument

function is 1.0. In the first position of Fig. 7, the instrument with such a function would record an intensity without absorption proportional to 5.6 and with absorption an intensity of 4.5. Thus  $\kappa_A^{\text{peak}} = 0.219$  compared to the true value 0.288. It is important to notice that in the absence of the wings in the instrument function, the situation is such that  $\kappa_A^{\text{peak}} = \kappa_T^{\text{peak}}$ ; the depression of the observed peak value of  $\kappa$  comes solely from the wings (for this special case). Moving the instrument function to position 2, we find that there would be a difference between the intensities recorded with and without absorbing atoms, even though there is no absorption at this frequency in the true spectrum. Finally, even with the instrument function moved outside the emission line there would be a difference recorded with and without absorption. The difference between cases 2 and 3 is that in position 2, the absorption signal is riding on top of the large signal produced by the emission line. Hence in an actual experimental situation, the observed absorption tends to zero towards the wings of the emission line, but may reappear more strongly when no longer masked by the strong signal from the emission line. For this, case  $I_0$  and  $I_{\text{abs}}$  in position 2 are 5.6 and 5.4, giving  $\kappa_A = 0.0345$ ; and in position 3, the intensities are 2.0 and 1.8 for  $\kappa_A = 0.104$ . This agrees qualitatively with the behavior of  $\kappa_A$  shown in Fig. 1.

Now the effect of a second emission line elsewhere in the pass band of this instrument may be understood. When the instrument function is centered on the emission line at the absorption frequency, the wings of the function are sensitive to the second emission line. This sensitivity has the effect of adding a constant intensity to the signal recorded with and without absorption, thus producing a further depression of  $\kappa_A$ .

Some special situations similar to those described above have been numerically computed for Gaussian emission and absorption lines and Airy functions. The recorded spectra were found to be extremely sensitive to the location of any "extra" emission lines. The closer the extra emission line was to the absorption line, the more was  $\kappa_A^{\text{peak}}$  depressed. These calculations were done for very specific cases, and the results will not be reproduced here.

### B. Fourier Expansion of the Absorption Integral

The convolution integral of Eq. (1) may be found explicitly as a double sum. We used this sum in evaluating some of the integrals, but of course this formulation does not apply to the constant-intensity case or the Voigt profiles in absorption. We use the well-known fact<sup>13</sup> that the Fourier transform of the convolution integral of two functions is just the product of the individual Fourier transforms of the functions. The Fourier transform  $G(y)$  of the Airy function  $g(\nu)$  has been given by Krebs and Sauer;<sup>11</sup> it may be written as

$$G(y) = 2\pi \frac{1-R}{1+R} \sum_{n=-\infty}^{\infty} R^{|n|} \delta(y + 2\pi n).$$

(The Fourier transform of a periodic function is a "row of delta functions.")

In order to find the Fourier transform of the absorbed intensity  $\mathcal{I}_{\text{abs}}(y)$ , we write

$$\begin{aligned} \mathcal{I}_{\text{abs}}(y) &= (2\pi)^{-1/2} \int_{-\infty}^{\infty} dx e^{ixy} e^{-x^2/\beta^2} e^{-\kappa e^{-x^2/\gamma^2}} \\ &= (2\pi)^{-1/2} \int dx e^{ixy} e^{-x^2/\beta^2} \sum_{m=0}^{\infty} \frac{(-\kappa)^m}{m!} e^{-mx^2/\gamma^2} \end{aligned}$$

$$= 2^{-1/2} \sum_{m=0}^{\infty} \frac{(-\kappa)^m}{m!} \frac{\beta\gamma}{(m\beta^2 + \gamma^2)^{1/2}} e^{-\beta^2 \gamma^2 y^2 / 4(m\beta^2 + \gamma^2)}$$

Here  $\beta$  and  $\gamma$  are the  $1/e$  widths of the emission and absorption lines.

The Fourier transform of the convolution integral (1) is then merely  $(2\pi)^{1/2}$  times the product of these two sums, and the inverse transform can be found readily. The result is

$$I_{\text{abs}}(x) = (\pi)^{1/2} \frac{(1-R)}{(1+R)} \beta\gamma \sum_{m=0}^{\infty} \frac{(-\kappa)^m}{m!(m\beta^2 + \gamma^2)^{1/2}} \\ \sum_{n=-\infty}^{\infty} R^{|n|} (\cos 2\pi n x) \exp[-(\pi n \beta \gamma)^2 / (\gamma + m\beta^2)].$$

This expression reduces to that found by Krebs and Sauer for the intensity transmitted by a Fabry-Perot in the absence of absorption, by taking only the  $m=0$  term in the sum over  $m$ . This procedure is equivalent to setting the exponential absorption term in Eq. (1) equal to 1. Under some conditions this series will converge rapidly.

The technique used above may be applied to any line shape for which the Fourier transform can be found. For instance, it leads to a very simple derivation of the formula found by Ballik<sup>14</sup> for an emission Voigt profile, since the Fourier transform of this profile is simply  $(2)^{-1/2} \exp(-a|y| - y^2/4)$ . Unfortunately there appears to be no simple expression for the Voigt profile in absorption, although the Lorentz profile in absorption can be treated fairly readily.

FOOTNOTES AND REFERENCES

\* Presented in part at the Philadelphia Meeting of the Optical Society of America, 8 Oct. 1965. J. Opt. Soc. Am. 55, 1584A (1965).

† Work supported in part by the U. S. Atomic Energy Commission.

§ Present address: State University of New York, Buffalo, New York 14214.

\*\* Work supported in part by the U. S. Advanced Research Projects agency.

1. Henry J. Kostkowski and Arnold M. Bass, J. Opt. Soc. Am. 46, 1060 (1956).
2. Thomas G. Kyle and Jay O. Green, J. Opt. Soc. Am. 55, 895 (1965).
3. Hyatt M. Gibbs and Robert J. Hull, Rb<sup>87</sup>-Rb<sup>87</sup> and Rb<sup>87</sup>-Cs<sup>133</sup> Spin-Exchange Cross Sections, Lawrence Radiation Laboratory Report UCRL-16785 (May 1966); to be submitted to Phys. Rev. H. M. Gibbs, Total Spin-Exchange Cross Sections for Alkali Atoms from Optical Pumping (Ph. D. thesis), Lawrence Radiation Laboratory Report UCRL-16034 1965 (unpublished).
4. Karl W. Meissner, J. Opt. Soc. Amer. 32, 185 (1942).
5. P. Jacquinot, Reports on Progress in Physics XXIII, 267 (1960).
6. See, for example: John Stone, Radiation and Optics (McGraw-Hill Book Co., New York, 1963), p. 411.
7. Joseph Winocur and Robert V. Pyle (Lawrence Radiation Laboratory), private communication, 1963. Since the effect was first noticed, a description of the work has appeared in J. Appl. Phys. 36, 2740 (1965).

Although no mention of the effect is made, absorption may be seen in the wings of the spectral profile shown in Fig. 3 of their paper.

8. Allan C. G. Mitchell and Mark. W. Zemansky, Resonance Radiation and Excited Atoms (Cambridge University Press, 1961) p. 101.
9. H. G. Kuhn and J. M. Vaughan, Proc. Roy. Soc. (London) 277, 297 (1963).
10. R. Minkowski and H. Bruck, Z. Physik 95, 299 (1935).
11. K. Krebs and A. Sauer, Ann. Physik 13, 359 (1953).
12. Hans Kopfermann and Günter Wessel, Z. Physik 130, 100 (1951).
13. Philip M. Morse and Herman Feshbach, Methods of Theoretical Physics (McGraw-Hill Book Company, New York, 1953) p. 483.

We have used the normalization of the Fourier integral given in this reference.

14. E. A. Ballik, Appl. Opt. 5, 170 (1966).

Table I. The ratio  $S_A/S_T$  of the apparent to true line intensities for various operating conditions. Finesse is 25. The true value  $\kappa_T^{\text{peak}}$  is 0.3. The apparent line intensity  $S_A$  includes the contribution from the tail.

$\Delta\nu/a_T$	$a_E$			
	$1.5 a_T$	$2.0 a_T$	$3.0 a_T$	Constant
0.438	2.03	1.46	1.11	0.977
4.38	27.3	21.5	14.6	0.908

Table II. Parameters to be used in Eq. (7) for generating correction factors to  $\kappa_A^{\text{peak}}$ . These values have been obtained for a finesse of 25, but apply with only a very small error to instruments with finesse between 15 and 40.

$\Delta\nu/a_T$	$a_E$	a	b	c
0.438	1.5 $a_T$	0.902	-0.012	-0.008
	2.0 $a_T$	0.885	-0.015	-0.013
	3.0 $a_T$	0.860	-0.019	-0.022
	constant	0.824	-0.025	-0.039
0.875	1.5 $a_T$	0.834	-0.023	-0.013
	2.0 $a_T$	0.806	-0.031	-0.019
	3.0 $a_T$	0.770	-0.039	-0.032
	constant	0.691	-0.061	-0.068
1.75	1.5 $a_T$	0.743	-0.043	-0.019
	2.0 $a_T$	0.697	-0.057	-0.029
	3.0 $a_T$	0.642	-0.074	-0.046
	constant	0.514	-0.120	-0.107
4.38	1.5 $a_T$	0.629	-0.074	-0.029
	2.0 $a_T$	0.554	-0.101	-0.044
	3.0 $a_T$	0.467	-0.133	-0.071
	constant	0.275	-0.213	-0.196

Table III. Values of the ratio of the true absorption width to the width of the fitted Gaussian,  $a_T/a_F$ , and of the ratio of the integral of the fitted Gaussian to the integral of the true line,  $S_F/S_T$ . These are tabulated for  $\Delta\nu/a = 0.438$  and  $N = 25$ , but the ratios are the same to within 4% for finesses between 15 and 40, except when overlap is a problem (low finesse, large  $a_T/a_E$ , as for  $N = 15$ ,  $a_T/a_E = 3.0$ ).

$a_E/a_T$	$\kappa_T^{\text{peak}}$					
	0.3		1.0		3.0	
	$a_T/a_F$	$S_F/S_T$	$a_T/a_F$	$S_F/S_T$	$a_T/a_F$	$S_F/S_T$
constant	0.884	0.922	0.887	0.877	0.855	0.741
3.0	0.866	0.985	0.875	0.946	0.865	0.827
2.0	0.843	1.04	0.856	1.01	0.864	0.900
1.5	0.807	1.11	0.826	1.07	0.851	0.968

Table IV. Values of the ratio of the true absorption width to the width of the fitted Gaussian,  $a_T/a_F$ , and of the ratio of the integral of the fitted Gaussian to the integral of the true line,  $S_F/S_T$ . These are tabulated for  $\Delta\nu/a_T = 0.875$  and  $N = 25$ , with approximately the same degree of accuracy as the values in Table III.

$a_E/a_T$	$\kappa_T^{\text{peak}}$					
	0.3		1.0		3.0	
	$a_T/a_F$	$S_F/S_T$	$a_T/a_F$	$S_F/S_T$	$a_T/a_F$	$S_F/S_T$
constant	0.788	0.857	0.793	0.788	0.765	0.612
3.0	0.752	1.01	0.768	0.943	0.772	0.774
2.0	0.707	1.13	0.730	1.05	0.753	0.885
1.5	0.626	1.32	0.664	1.21	0.713	1.01

## FIGURE LEGENDS

- Fig. 1. The true and apparent absorption coefficients when the Fabry-Perot has a finesse of 50 and  $\Delta\nu/a_T = 0.438$ . The abscissae are in frequency units of one free spectral range. The circles indicate the points for which the integrals were evaluated.
- Fig. 2. Experimentally observed absorption in the cesium  $D_1$  line ( $\lambda = 8944 \text{ \AA}$ ) when the Fabry-Perot has a finesse of 50 and a 8-mm spacer. Each broad peak is actually double due to the small hyperfine splitting in the  $6^2P_{1/2}$  state. The dip in the record near the center of the pattern is the zero of light intensity.
- Fig. 3. Maximum excursions in the ratio  $\kappa_A^{\text{peak}}/\kappa_T^{\text{peak}}$ . Values of this ratio lie on smooth curves inside these extremes when  $\Delta\nu/a_T$  equals 0.875 or 1.75 and for other emission widths.
- Fig. 4. The ratio  $a_A/A_T$  versus the instrument parameter  $\Delta\nu/a_T$  when  $\kappa_T^{\text{peak}} = 0.3$ . The curves rise so steeply that values of  $a_A/a_T$  are very large for  $\Delta\nu/a_T = 4.38$ .
- Fig. 5. These curves show the agreement between the fitted Gaussian  $\kappa_F$  and the apparent profile  $\kappa_A$ . The true profile  $\kappa_T$  is shown for comparison. For these curves the operating conditions are  $\Delta\nu/a_T = 0.438$ ,  $N = 25$ , and  $a_E/a_T = 2.0$ .
- Fig. 6. The apparent Voigt and Gaussian profiles computed with  $\Delta\nu/a_T = 0.438$ ,  $N = 25$ ,  $\kappa_T^{\text{peak}} = 0.3$  and constant intensity emission source.

Fig. 7. A schematic representation of three stages in the development of an absorption spectrum. Details are discussed in Appendix A.

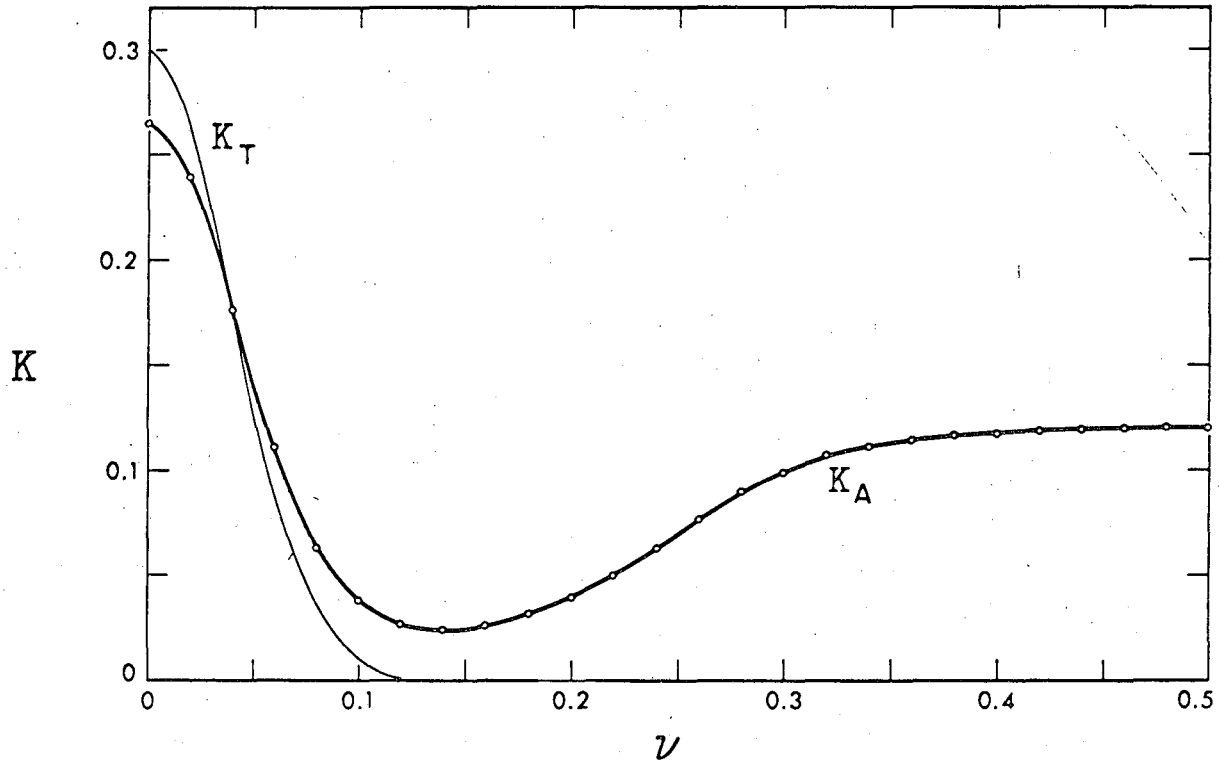
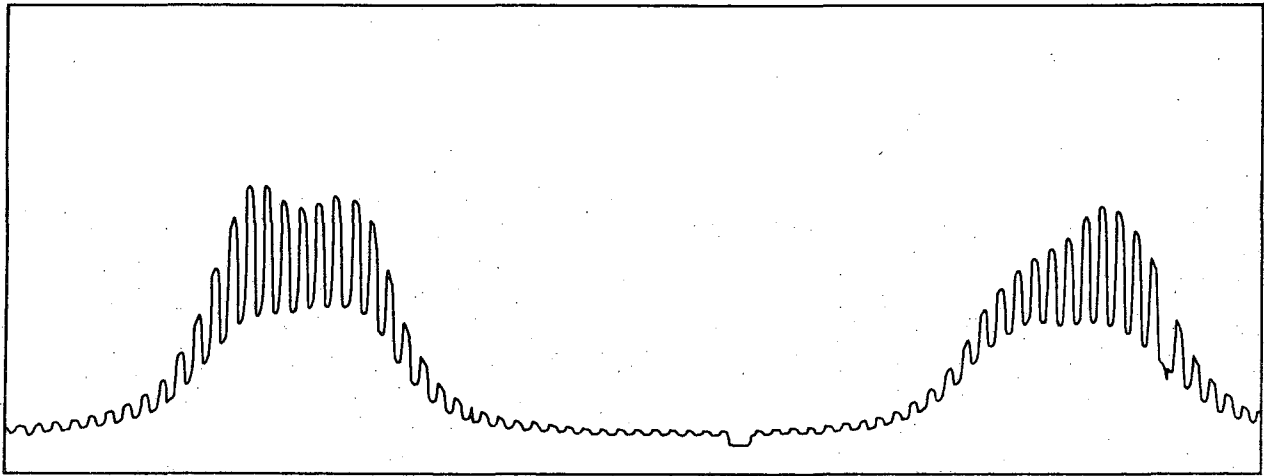


Fig. 1

MUB-7944-A



MUB-10573

Fig. 2

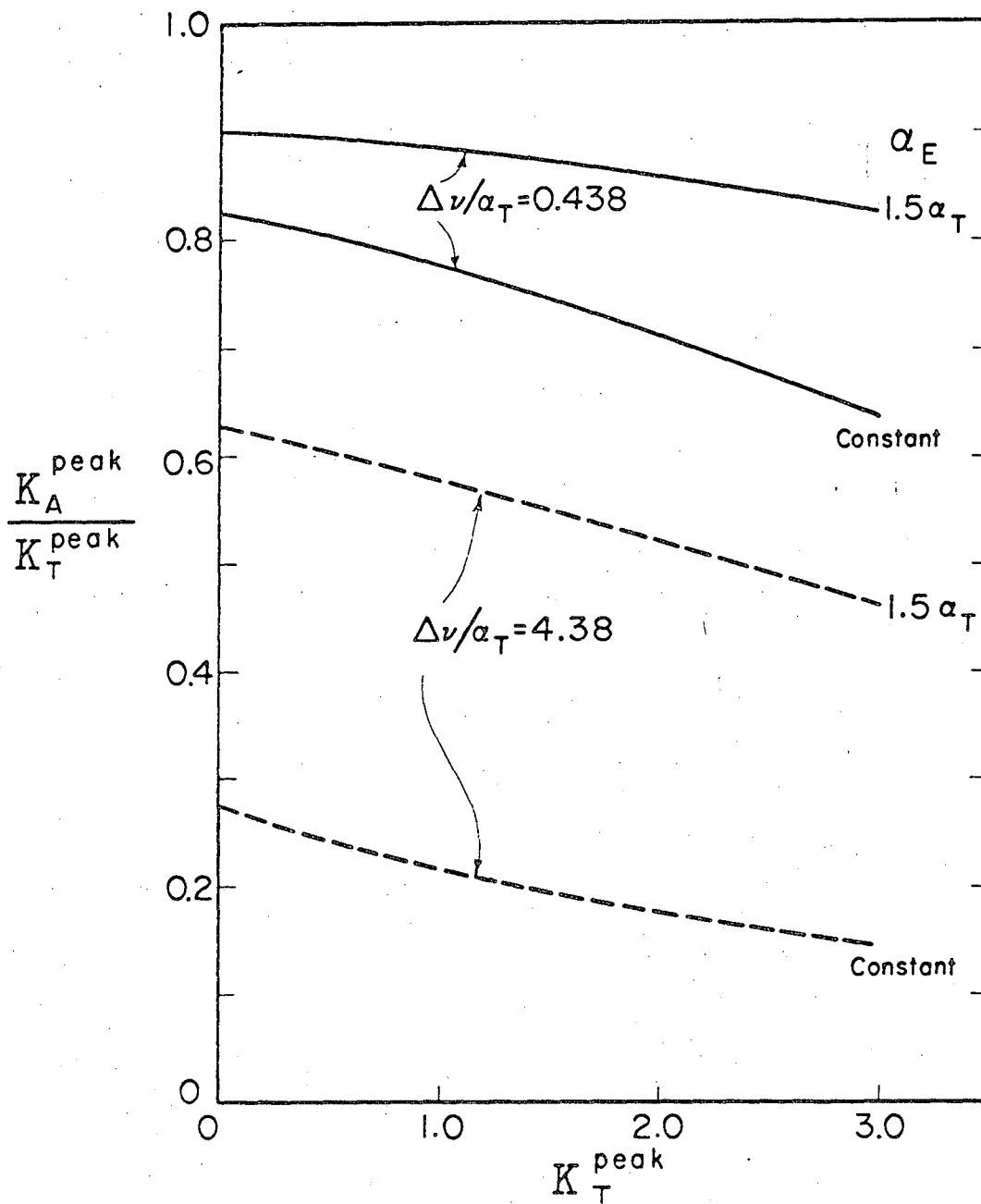
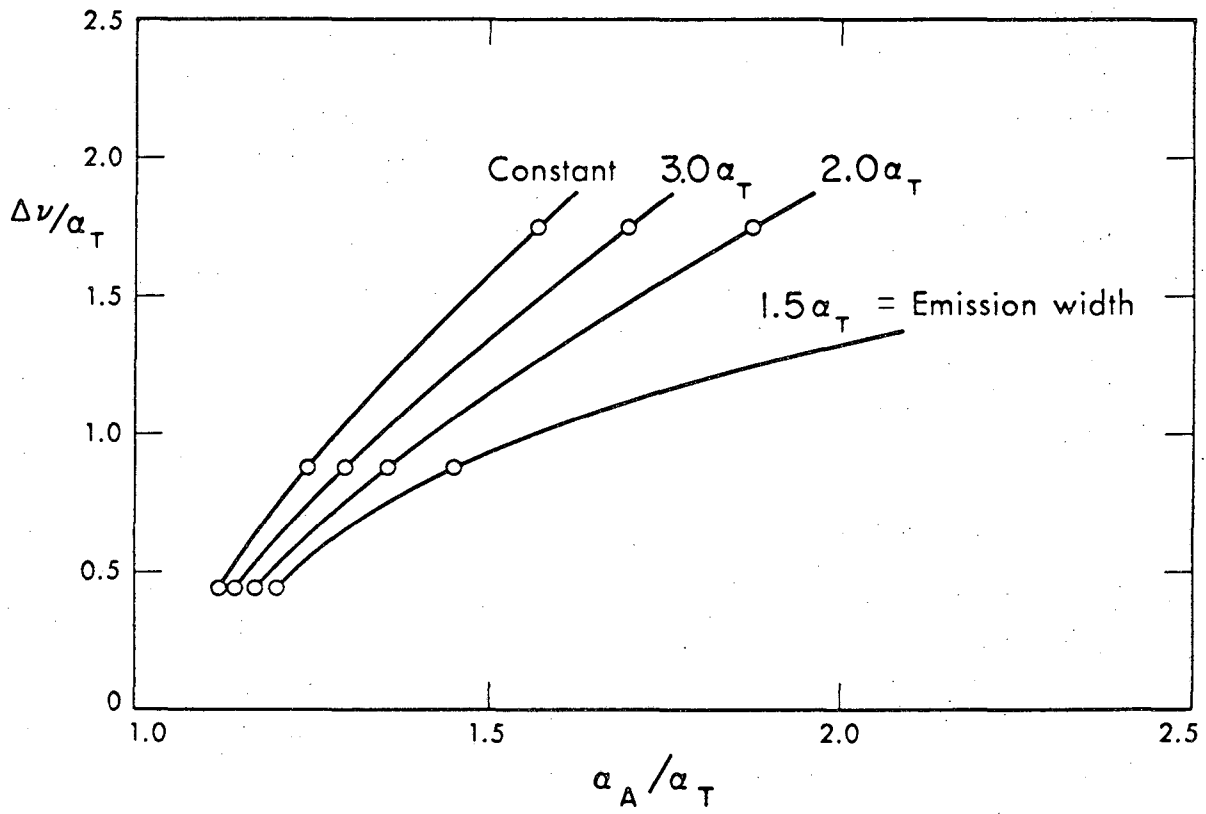


Fig. 3

MUB-7946-A



MUB-7947-A

Fig. 4

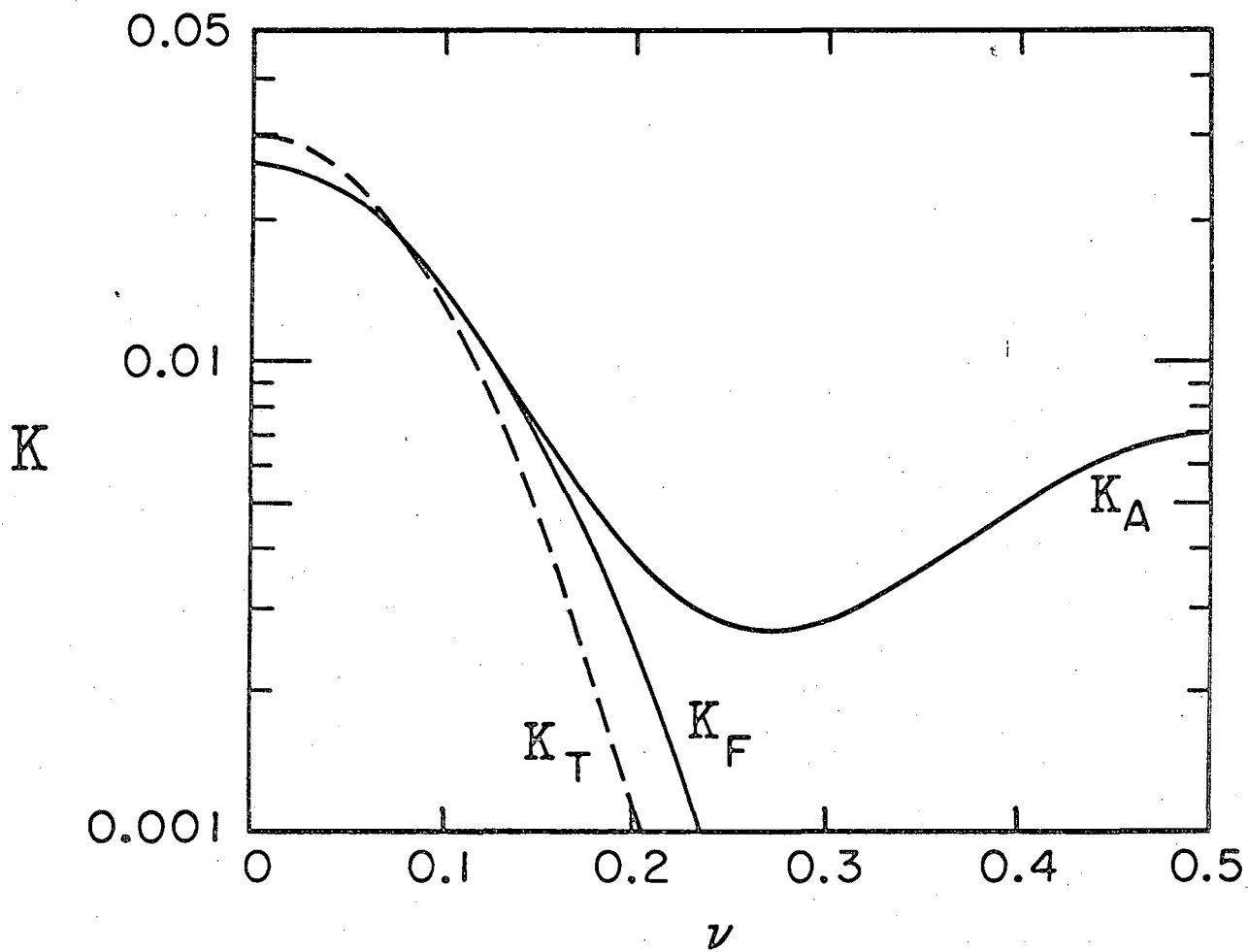


Fig. 5

MUB-10789

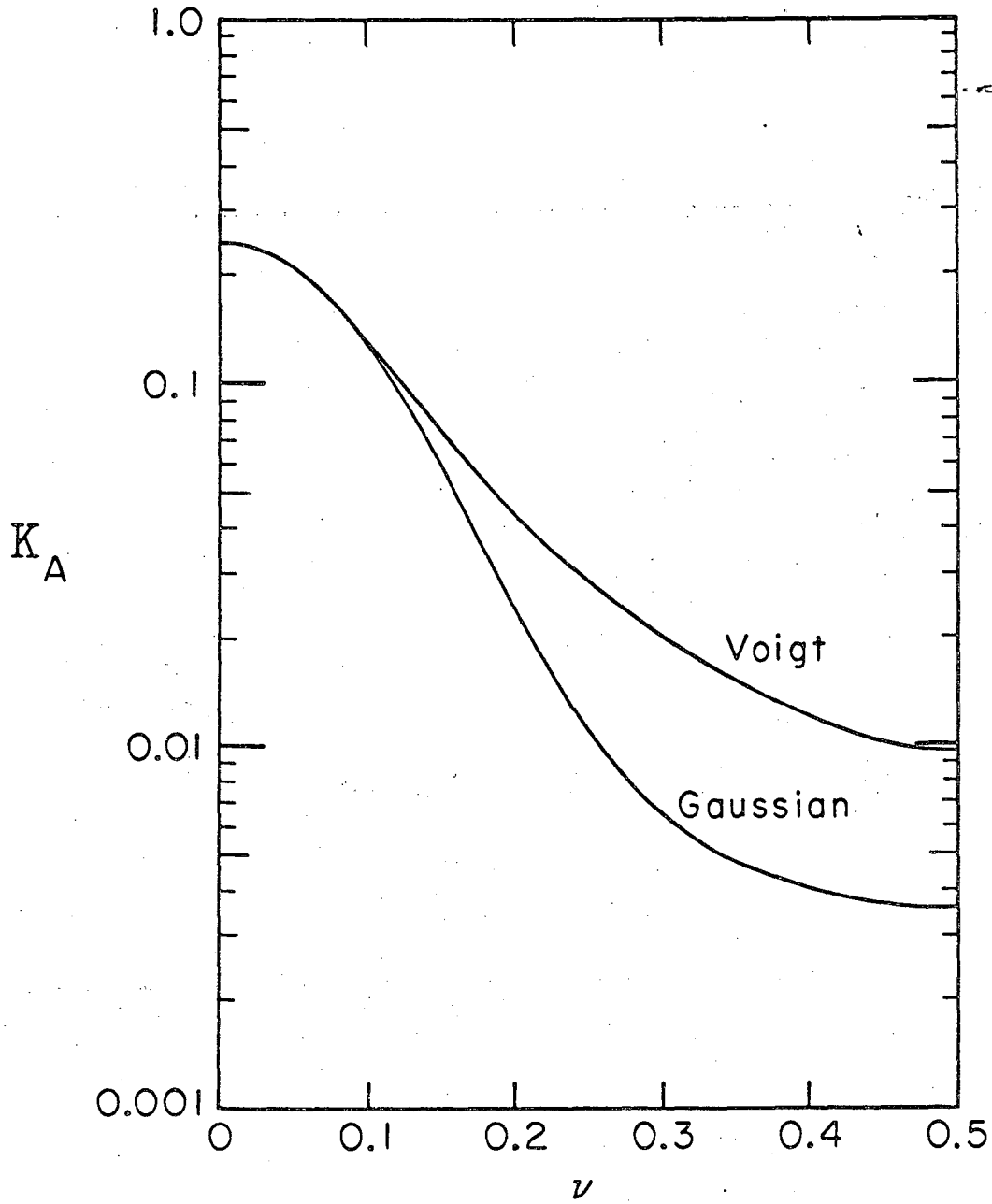
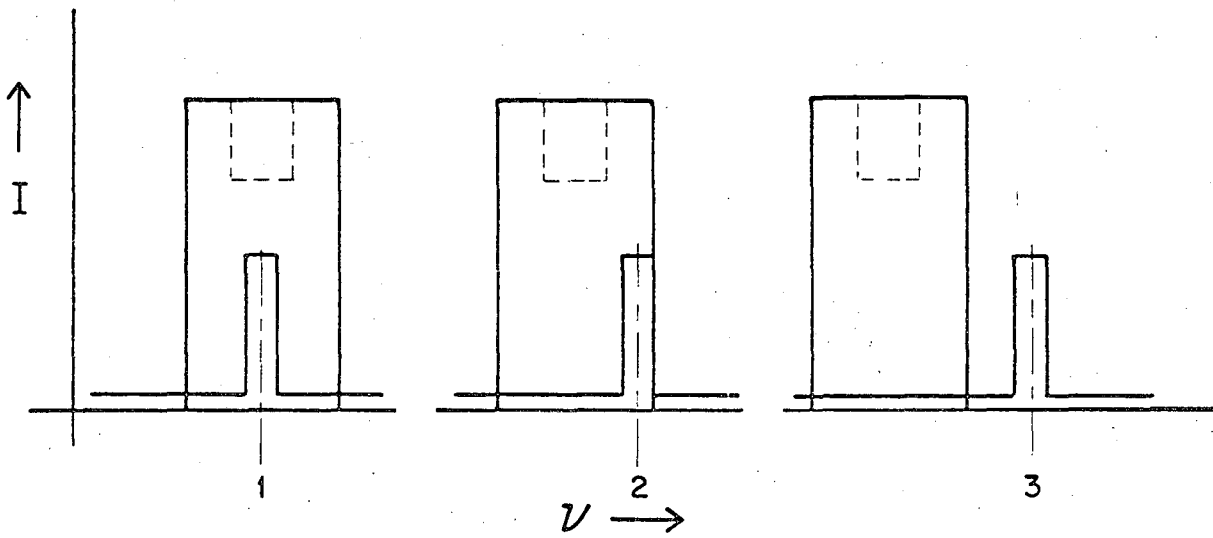


Fig. 6

MUB-10790



MUB-7945-A

Fig. 7

This report was prepared as an account of Government sponsored work. Neither the United States; nor the Commission, nor any person acting on behalf of the Commission:

- A. Makes any warranty or representation, expressed or implied, with respect to the accuracy, completeness, or usefulness of the information contained in this report, or that the use of any information, apparatus, method, or process disclosed in this report may not infringe privately owned rights; or
- B. Assumes any liabilities with respect to the use of, or for damages resulting from the use of any information, apparatus, method, or process disclosed in this report.

As used in the above, "person acting on behalf of the Commission" includes any employee or contractor of the Commission, or employee of such contractor, to the extent that such employee or contractor of the Commission, or employee of such contractor prepares, disseminates, or provides access to, any information pursuant to his employment or contract with the Commission, or his employment with such contractor.

